Published in final edited form as:
Acta Biomater. 2014 January ; 10(1): . doi:10.1016/j.actbio.2013.09.028.

Effects of clodronate and alendronate on osteoclast and osteoblast co-cultures on silk-hydroxyapatite films

Rebecca S. Hayden[a], **Moritz Vollrath**[a], and **David L. Kaplan**[a,*]

[a]Department of Biomedical Engineering, 4 Colby St., Tufts University, Medford, Massachusetts 02155, USA

Abstract

The goal of this study was to explore the effects of osteoporosis-related therapeutics on bone remodeling *in vitro*. A previously established bone-tissue mimetic system consisting of silk protein biomaterials in combination with hydroxyapatite and human cells was used for the study. Silk-hydroxyapatite films were pre-complexed with the non-nitrogenous bisphosphonate clodronate or the nitrogenous bisphosphonate alendronate and cultured with THP-1 human acute monocytic leukemia cell line-derived osteoclasts, human mesenchymal stem cell derived-osteoblasts, or a direct co-culture of the two cell types. Metabolic activity, calcium deposition, and alkaline phosphatase activity were assessed over 12 weeks, and reconstructed remodeled biomaterial surfaces were also evaluated for quantitative morphological changes. Increased metabolic activity and increased roughness were found on the clodronate-complexed biomaterial substrates remodeled by osteoblasts and co-cultures of osteoblasts with osteoclasts, even at doses high enough to cause a 90 percent decrease in osteoclast metabolic activity. Films complexed with low doses of alendronate resulted in increased metabolic activity and calcium deposition by osteoblasts, while higher doses were similarly toxic among osteoclasts, osteoblasts, and cocultures. These results point to the utility of these well-defined bone-mimetic *in vitro* cultures as useful screens for therapeutics for bone-related diseases, particularly with the ability to conduct studies for extended duration (here for 12 weeks) and with pre-complexed drugs to mimic conditions found *in vivo*.

Keywords

osteoporosis; co-culture; bisphosphonates; silk

1. Introduction

Bisphosphonates are the current standard of care for osteoporosis, but debate remains regarding which patients should be treated. Bisphosphonates have positive effects on bone mineral density, as well as reducing wrist and spine fractures, but prevention of hip fractures has not been as clearly demonstrated [1]. Rare but serious adverse events such as jaw necrosis and atypical femoral fractures are associated with bisphosphonate use, and the

[*]*Address correspondence to:* David L. Kaplan, Ph.D., Department of Biomedical Engineering, Tufts University, 4 Colby St., Medford, MA 02155, Phone: +1-617-627-3251, david.kaplan@tufts.edu, Fax: +1-617-627-3231.

mechanisms for these events are not well understood [2,3]. The benefits and drawbacks of long-term bisphosphonate use are particularly poorly understood, which is problematic for a chronic condition such as osteoporosis [4–6].

Because of their strong affinity for calcium, bisphosphonates efficiently bind to bone upon ingestion where they are eventually taken up by osteoclasts during bone remodeling, resulting in reduced bone resorption. The primary mechanism of action differs between the two classes of bisphosphonates. Non-nitrogenous bisphosphonates are metabolized by osteoclasts resulting in toxic adenosine triphosphate analogs and subsequent osteoclast apoptosis [7]. Nitrogenous bisphosphonates result in reduced osteoclast activity and osteoclast apoptosis through inhibition of the enzyme farnesyl diphosphate synthase (FPPS), which inhibits protein prenylation and interferes with the ruffled border that osteoclasts must maintain in order to resorb bone [8].

While most studies have focused on the effects of bisphosphonates on osteoclasts, some studies have investigated their effects on osteoblasts and osteoblast-like cells [9–13]. In a variety of systems, including animal models of osteogenesis and those with primary human osteoblasts and osteoblasts derived from human mesenchymal stem cells (hMSCs), bisphosphonates promoted the proliferation, differentiation, and activity of osteoblasts at low doses, and had the opposite effect at higher doses [14]. The mechanism for increased osteoblast survival was extracellular signal-related kinase (ERK) activation, and was independent of bisphosphonate class and osteoclast inhibition [15]. However, *in vitro* studies of bisphosphonates have generally been of short duration (less than 2 weeks), and bisphosphonates have routinely been administered in cell culture media. While some studies have investigated the effects of bisphosphonates incorporated into mineral substrates of hydroxyapatite or octacalcium phosphate on co-cultures of osteoblasts and osteoclasts for one to two weeks, the long-term sustainability and cellular effects of such systems require further study [16–18]. The nature of osteoporosis as a chronic condition and bisphosphonates as agents with long half-lives *in vivo* particularly necessitate such long-term studies.

The objective of the present study was to develop and utilize an *in vitro* bone mimetic model to address the current minimal understanding of the effects of bisphosphonates on osteoblasts and other cell types in long-term culture. To address this objective, monocultures of bone marrow-derived hMSC osteoblasts and THP-1 acute monocytic leukemia cell-derived osteoclasts, as well as co-cultures of the two cell types, were maintained for 12 weeks on silk hydroxyapatite (HA) biomaterial films with sequestered alendronate or clodronate. Standard measures of metabolic activity and differentiation were monitored throughout the experiment. Additionally, digital 3D images of remodeled film surfaces were reconstructed using surface metrology software and scanning electron microscopy (SEM) to quantify biomaterial remodeling (Figure 1). This work points to the use of *in vitro* disease models for increased understanding of drug effects, here particularly focused on bone-related diseases in long term culture, as well as appropriate sequestration of the drugs to provide more realistic systems to mimic physiological conditions.

2. Materials and Methods

2.1 Cell culture

Unless otherwise noted, cell culture reagents were purchased from Life Technologies (Grand Island, NY). hMSCs were isolated from bone marrow aspirate (Lonza, Walkersville, MD) as described previously [19]. Briefly, aspirate from a male donor under 25 years old was combined with hMSC proliferation medium (MEM α with 10% FBS, 1% antibiotic/antimicotic, 1% non-essential amino acids (NEAA)) and cultured at 37°C with 5% CO_2 in a

humidified environment. Flasks were rocked every day to allow hMSCs to adhere and media was added every 3–4 days until hMSCs reached 80% confluence. hMSCs were used at passage 1 or 2. THP-1 cells (ATCC, Manassas, VA) were maintained in proliferation medium (RPMI 1640 supplemented with 10% FBS, 1% antibiotic/antimycotic, and 1% NEAA) prior to seeding. 15,000 cells per cm^2 were seeded onto films (50% hMSCs and 50% THP-1 cells for co-cultures) in a 50 μl drop and incubated for 2 hours to allow attachment. Following seeding, all cultures were maintained in the same medium, a half and half mixture of RPMI 1640 and MEM α supplemented with 10% FBS, 1% antibiotic/antimycotic, 1% NEAA, 100 nM dexamethasone (Sigma Aldrich, St. Louis, MO), 10 mM B-glycerol phosphate (Sigma Aldrich, St. Louis, MO), and 0.05 mM ascorbic acid (Sigma Aldrich, St. Louis, MO) (for osteoblast differentiation, as described previously [20]), and 40ng/ml phorbol 12-myristate 13-acetate (PMA) (Sigma Aldrich, St. Louis, MO) and 10 ng/ml receptor activator of nuclear factor kappa-B ligand (RANKL) (for osteoclast differentiation, as described previously [21]) with medium changes every 3–4 days.

2.2 Silk film preparation and drug loading

Aqueous silk solution was prepared as described previously [22]. Briefly, cocoons of *Bombyx mori* were cut to pieces approximately 1.5 cm^2 and boiled for 30 minutes in water containing 0.02 M Na_2CO_3, and then rinsed thoroughly with water to remove sericin. The remaining silk fibroin was then dried and dissolved in 9.3 M LiBr (Sigma Aldrich, St. Louis, MO) solution at 60°C for 4 hours. This solution was dialyzed in distilled water using a Slide-A-Lyzer dialysis cassette (MWCO 3,500, Thermo Fisher Scientific, Rockford, IL) for 2 days resulting in an 8% silk solution. Silk-HA films were prepared using a 5.0 % (w/v) silk solution mixed with 5.47 mg/ml synthetic HA powder (Sigma Aldrich, St. Louis, MO). For each film 100 μl of this freshly prepared dispersion was cast into a well in the lid of a 96 well plate. The silk-HA dispersion was mixed periodically to maintain a homogenous dispersion and the same HA content in each film. The films were covered and dried for 24 h at room temperature and then water annealed for 24 h using a desiccator as described previously [23]. The silk-HA films were then soaked in solutions of alendronate sodium trihydrate or clodronic acid disodium salt (Sigma Aldrich, St. Louis, MO) for 48 h at 37°C. Target quantities of drugs to be loaded on the silk-HA films were selected based on the literature, and pilot studies were carried out to determine the percentage of bisphosphonate that bound to the films. For the long-term cultures, higher targets were selected for osteoclast cultures and co-cultures, while lower targets were selected for mono-cultures of osteoblasts. Drug loading is reported as μg per silk-HA film (8 mm diameter). Following loading, films were sterilized by autoclaving and incubated overnight in medium prior to cell seeding.

2.3 Measurement of calcium release

Silk-HA films were incubated in PBS at 37°C. Every 24 hours the films were transferred to fresh PBS and calcium release was quantified using the Stanbio (Boerne, TX) calcium cresolphthalein complexone assay according to the manufacturer's protocol. Absorbance was measured at 550 nm.

2.4 Quantification of bisphosphonate concentrations

Following soaking, the concentrations of bisphosphonates remaining in solution were measured to calculate the amount of drug sequestered on the films. Clodronate concentration was determined by taking 100 μl of the reserved soaking solution, adding 30 μl of 50 mM $FeCl_3$-solution in 2M $HClO_4$, and measuring the absorbance at a wavelength of 294 nm as described previously [24]. Alendronate concentration was determined using ninhydrin as described previously [25]. Reserved soaking solution was added to 0.5 ml 0.01 M $NaHCO_3$

and 2.5 ml 0.2 % (w/v) ninhydrin solution in methanol. After the solution was heated for 20 minutes in a water bath at 90°C the flasks were cooled and the volume was brought up to 10.0 ml. Samples of 100 μl were used to measure the absorbance at 568 nm.

2.5 Metabolic activity measurement

Metabolic activity was measured using Alamar Blue (Life Technologies, Grand Island, NY). The films were rinsed in PBS and transferred to a sterile 48 well plate for each Alamar Blue assay to ensure that only the metabolic activity of cells growing on the films was measured. Light exposure was minimized during all working steps. The Alamar Blue solution was prepared by mixing the calculated amount of co-culture media with 10 % Alamar Blue and 500 μl of the freshly prepared solution was added to each well and films incubated for 150 minutes. Fluorescence of 100 μl aliquots was measured with excitation at 560 nm and emission at 590 nm. Background fluorescence from the Alamar Blue solution alone was subtracted.

2.6 Calcium deposition analysis

Samples for calcium analysis were rinsed in PBS and kept at −20°C prior to testing. Films were incubated in 5% trichloroacetic acid for 30 minutes. Following centrifugation the calcium content of the supernatant was assessed using the Stanbio (Boerne, TX) calcium cresolphthalein complexone assay according to the manufacturer's protocol. Absorbance was measured at 550 nm.

2.7 SEM

Films were incubated in ddH_2O overnight at 4°C in order to remove cells. Samples were coated for 90 seconds at 18 mA using the sputter coater SC7600 (EMITech, Fall River, MA). Samples were imaged using a Zeiss EVO MA10 SEM with the SE1 detector (Oberkochen, Germany). From each sample four different areas were imaged. Eucentric images were taken from tilt angles of 0 degrees and 8 degrees at 2000× magnification.

2.8 Surface metrology

MeX software (Alicona, Graz, Austria) was used for surface metrology. MeX surface metrology software allows a digital 3D model of the surface to be generated from SEM images taken at any magnification for subsequent surface metrology of individual features or large areas [26–29]. 3D surfaces were generated from eucentric image pairs with an eight degree tilt differential and area analysis was performed using a reference plane generated from all points and a filter to exclude waviness. The measure of surface roughness presented here is the developed interfacial ratio, which quantifies the increase in surface area as a result of roughness.

2.9 Statistical analysis

All values are presented as mean +/− SD. Statistical signification was determind by tukey’s HSD post-hoc ANOVA using R: A Language and Environment for Statistical Computing.

3. Results

3.1 Film characterization

In order to verify that HA remained entrapped in the silk-HA films throughout culture, calcium release studies of silk-HA films were conducted. The cumulative calcium release at 10 days accounted for 0.58% of the 0.547 mg total HA per film. Drug loading efficiency for the long term study is shown in Table 1. On average, 18% of the clodronate in the film soaking solution was bound to the silk-HA films. For alendronate the average was 29%.

3.2 Metabolic activity

For the one week cultures, metabolic activity was measured by Alamar Blue at 1, 3, 4, 5, 6, and 7 days (Figure 2). At the highest dose of clodronate (262 μg per film) no osteoclast metabolic activity could be measured at days 6 and 7, but about 80% of control metabolic activity was maintained in osteoblasts and co-cultures at the same dose. At the highest dose of alendronate (70 μg per film) metabolic activity was abolished by day 6 for all cultures. However, for the 54 μg dose osteoblasts maintained 10% of control metabolic activity and co-cultures maintained 22% of control metabolic activity while osteoclasts maintained only 2% of control metabolic activity.

For the longer term (12 week cultures) metabolic activity was measured by Alamar Blue at 1, 4, 6, 8, 10, and 12 weeks (Figure 3). Osteoclasts cultured on films loaded with clodronate demonstrated increased metabolic activity of up to 215% of the metabolic activity of osteoclast cultured on control silk-HA films at week 1. Metabolic activity of osteoclasts cultured on clodronate-loaded films decreased throughout the 12 weeks and was below 10% of control metabolic activity at weeks 10 and 12 for films with 119 μg clodronate, while osteoclasts on films with 64 μg clodronate had a metabolic activity of 13% of the control cells by week 12. Osteoblast metabolic activity was not significantly reduced throughout the experiment. At week 12 osteoblasts on films with 18 μg clodronate had a metabolic activity of 106% of the control metabolic activity, while osteoblasts on films with 63 μg had a metabolic activity of 107% of the control metabolic activity. The average metabolic activities of co-cultures on films with 52 μg clodronate and 113 μg clodronate were greater than 100% at each time point.

Osteoclasts cultured on films with alendronate also exhibited a transient increase in metabolic activity at 1 week of up to 150% of control cultures. As with clodronate, metabolic activity of osteoclasts cultured on films loaded with alendronate decreased over 12 weeks, down to 7% of the control for cells cultured on films with 36 μg alendronate at week 12. While a very low dose of 2.4 μg alendronate per silk film resulted in increased osteoblast metabolic activity at some time points, 3.8 μg alendronate per silk film resulted in osteoblast metabolic activity of 76% to 98% of control metabolic activity after week 1. Co-cultures on films with 12 and 19 μg alendronate had metabolic activity reduced to 21% and 19% of control metabolic activity at the first time point. At the lower dose metabolic activity increased over 12 weeks to 94% while at the higher dose metabolic activity was 64% of the control by week 12.

3.3 Calcium content

Calcium content of the films was quantified at 4, 8, and 12 weeks (Figure 4). In general, calcium content increased throughout the experiment in the osteoblast and co-culture groups. Clodronate did not significantly alter calcium content except for osteoblasts at the 8 week time point, when osteoblasts cultured on 18 μg clodronate films deposited more calcium than osteoblasts on 63 μg clodronate films. Low doses of alendronate increased calcium content by osteoblasts, but the higher doses in the co-culture group resulted in a dose-dependent decrease in calcium content of up to 74% for the highest dose at week 12.

3.4 Surface metrology

The 150 μm by 100 μm biomaterial (silk-HA) surfaces were reconstructed from the films remodeled in culture for 4, 8, and 12 weeks (Figure 5). The interfacial ratio (Sdr) is the percent increase in surface area due to roughness. Among films remodeled by osteoclasts, films loaded with 64 μg clodronate had a significantly increased Sdr at 8 weeks. In osteoblast cultures and co-cultures the Sdr was significantly higher at 8 and 12 weeks on clodronate-loaded films. Alendronate-loaded films remodeled by osteoclasts had

significantly increased Sdrs at 4 and 8 weeks. At low doses in osteoblast cultures trends were towards increased Sdrs. At the 12 μg dose in co-culture the Sdr was significantly increased at 4 weeks, but the higher dose at later time points trended towards a decrease in the Sdr.

4. Discussion

Previous studies have demonstrated that silk biomaterials support long-term tissue engineering of bone and that silk biomaterials can be used to study bone remodeling. For example, silk sponges have been used for bone tissue engineering with and without hMSCs *in vivo* in various animal models, as well as to study cancer metastasis and osteoarthritis [30–35]. We have also studied the degradation of bone on silk films by osteoclasts *in vitro* and used SEM-based surface metrology to measure changes in silk film remodeling by hMSCs expressing tethered parathyroid hormone and glucose-dependent insulinotropic peptide (unpublished results) [21]. In all of these prior studies, the silk-bone systems have proven to be relevant model tissue systems for studying human bone formation and function. In the present study we generated silk-HA films which we then preloaded with various concentrations of bisphosphonates. Cultures of osteoclasts, osteoblasts, and co-cultures of osteoclasts and osteoblasts were maintained on the films out to 12 weeks, and metabolic activity, calcium deposition, and surface remodeling were monitored.

In most *in vitro* studies of bisphosphonates, the drug is added to the media. Silk-HA films with pre-bound bisphosphonates are more representative of *in vivo* conditions for several reasons. *In vivo*, bisphosphonates are quickly chelated to HA in bone [7]. Statins and nitrogenous bisphosphonates act on the same pathway, but statins lack affinity for calcium which contributes to the differing effects of the drugs [36]. As a result, bisphosphonates suspended in culture medium may affect osteoblasts differently than those sequestered on a calcium-rich material [37]. Additionally, films enable long term culture as opposed to more traditional cell culture on tissue culture plastic. Since osteoporosis is a chronic condition and bisphosphonates are characterized by a long half-life in humans, the short duration of experiments possible on tissue culture plastic may not provide meaningful information about the interactions of bone cells with bisphosphonates *in vivo* [38]. Finally, films provide a surface onto which extracellular matrix is deposited and remodeled over long culture periods, resulting in a pseudo-3D environment which is suitable for SEM imaging and surface metrology.

The bisphosphonate doses selected for this study were based on the literature as well as pilot studies [37,39–44]. For the 12 week cultures doses were lower than for the 7 day cultures to avoid immediate cell death. Doses for osteoclast cultures were selected to significantly reduce metabolic activity. Doses for osteoblast cultures were selected to enhance osteoblast differentiation. Intermediate doses were selected for co-cultures. While the use of different doses for different cell types prevents some types of direct comparisons, it facilitates other comparisons. For example, the different concentrations chosen demonstrated that clodronate promoted osteoblast metabolic activity and matrix deposition even at concentrations high enough to vastly reduce osteoclast activity. In contrast, the positive effects of alendronate on osteoblasts occurred only at very low doses.

The differences in osteoblast response to clodronate and alendronate may be due to the different mechanisms of action of nitrogenous and non-nitrogenous bisphosphonates, shown in Table 2. While the pro-survival effects of bisphosphonates on osteoblasts are believed to be independent of drug class, toxicity is not independent of drug class. Nitrogenous bisphosphonates cause apoptosis in various cell types at concentrations similar to those that cause osteoclast apoptosis, and by the same mechanisms [41]. Nitrogenous bisphosphonates

also inhibit mineralization by a separate mechanism than the inhibition of protein prenylation that causes apoptosis [41]. However, while non-nitrogenous bisphosphonates are less potent than nitrogenous bisphosphonates, previous studies have reported that osteoblast and osteoclast apoptosis occurred at similar concentrations of non-nitrogenous bisphosphonates [14]. It is hypothesized that *in vivo* osteoclasts experience a higher bisphosphonate concentration than osteoblasts, and that this may mitigate the osteoblast apoptosis demonstrated *in vitro*. While this may explain the high tolerance of osteoblasts for clodronate in this study, alendronate was similarly toxic to osteoblasts and osteoclasts in our model. Since alendronate is known to bind more strongly to calcium than clodronate, it seems likely that differences between the mechanisms of toxicity of clodronate and alendronate may be responsible for these findings.

In addition to measuring calcium deposition, we quantified the Sdr of remodeled films. Since the Sdr is a measurement of increased surface area as a result of roughness, its increase does not necessarily represent an increase in deposited calcium. Resorption also increases the surface area, as does the formation of fewer, larger mineral deposits. Assessment of surface morphology provides additional information in co-cultures were the continuous deposition and resorption of mineral is not adequately described by the net calcium deposition.

We attempted to measure alkaline phosphatase (ALP) activity at 4, 8, and 12 weeks (data not shown). Clodronate did not significantly alter ALP activity except for the osteoblast cultures at the 12 week time point, where osteoblasts cultured on 18 μg clodronate films had increased ALP activity. Alendronate resulted in a dose-dependent decrease in ALP expression in the treated co-culture groups of up to 87% at the 4 week time point. However, the interpretation of this data is complicated by the fact that ALP could not be normalized to osteoblast cell number. Additionally, previous studies have generally measured ALP activity at earlier time points, complicating comparisons with prior work.

While most *in vitro* studies of bisphosphonates have been of short duration, cells in the present study were maintained for 12 weeks. While osteoclast metabolic activity decreased throughout the culture period, metabolic activity of osteoblasts exposed to alendronate increased. While the mechanism for this difference is unknown, it points to the importance of long-term studies to understand the effects of bisphosphonates.

5. Conclusions

We have shown that silk-HA films support the long-term culture of osteoblasts and osteoclasts, and that the addition of the bisphosphonates clodronate and alendronate alter metabolic activity, calcium deposition, ALP activity, and remodeling measured by surface metrology. Additionally, in this bone tissue model clodronate supported increased osteoblast activity even at concentrations that vastly diminished osteoclast activity, while alendronate did not. Non-nitrogenous bisphosphonates have largely been eschewed in favor of the more recently developed nitrogenous bisphosphonates which have a higher activity and thus require lower doses. However, clinical trials of bisphosphonates tend to compare the drugs to placebos and calcium supplementation rather than other bisphosphonates, resulting in a lack of information regarding differences in fracture prevention and adverse events between bisphosphonates [45]. This work points towards the utility of tissue engineered models of bone remodeling to studying the long-term effects of drugs on human cells. While bisphosphonates were chosen for this study because they act locally on bone, combination of tissue engineered bone remodeling models with *in vitro* models of other organs such as the liver and kidney, and validation against the current rodent and large animal models used in

osteoporosis therapy may facilitate studies of therapies with more complex mechanisms of action in the future.

Acknowledgments

This work wasfunded by NIH grant number P41 EB002520 for the Tissue Engineering Resource Center. The funding source had no role in study design; in the collection, analysis and interpretation of data; in the writing of the report; or in the decision to submit the paper for publication.

References

1. Boonen S, Laan RF, Barton IP, Watts NB. Effect of osteoporosis treatments on risk of non-vertebral fractures: review and meta-analysis of intention-to-treat studies. Osteoporos Int. 2005; 16:1291–1298. [PubMed: 15986101]
2. Schilcher J, Michaëlsson K, Aspenberg P. Bisphosphonate use and atypical fractures of the femoral shaft. N Engl J Med. 2011; 364:1728–1737. [PubMed: 21542743]
3. Cartsos VM, Zhu S, Zavras AI. Bisphosphonate use and the risk of adverse jaw outcomes: a medical claims study of 714,217 people. J Am Dent Assoc. 2008; 139:23–30. [PubMed: 18167381]
4. Whitaker M, Guo J, Kehoe T, Benson G. Bisphosphonates for osteoporosis--where do we go from here? N Engl J Med. 2012; 366:2048–2051. [PubMed: 22571168]
5. Black D, Bauer D. Continuing bisphosphonate treatment for ssteoporosis—for whom and for how long? N Engl J Med. 2012; 366:2051–2053. [PubMed: 22571169]
6. Abrahamsen B. Are long-term bisphosphonate users a reality? Dose years for current bisphosphonate users assessed using the danish national prescription database. Osteoporos Int. 2012:10–13.
7. Rodan GA, Fleisch HA. Bisphosphonates: mechanisms of action. J Clin Invest. 1996; 97:2692–2696. [PubMed: 8675678]
8. Kimmel DB. Mechanism of action, pharmacokinetic and pharmacodynamic profile, and clinical applications of nitrogen-containing bisphosphonates. J Dent Res. 2007; 86:1022–1033. [PubMed: 17959891]
9. Nishikawa M, et al. Bisphosphonates act on osteoblastic cells and inhibit osteoclast formation in mouse marrow cultures. Bone. 1996; 18:9–14. [PubMed: 8717530]
10. Tenenbaum HC, Torontali M, Sukhu B. Effects of bisphosphonates and inorganic pyrophosphate on osteogenesis in vitro. Bone. 1992; 13:249–255. [PubMed: 1637572]
11. Sahni M, Guenther HL, Fleisch H, Collin P, Martin TJ. Bisphosphonates act on rat bone resorption through the mediation of osteoblasts. J Clin Invest. 1993; 91:2004–2011. [PubMed: 8486770]
12. Ohe J-Y, Kwon Y-D, Lee H-W. Bisphosphonates modulate the expression of OPG and M-CSF in hMSC-derived osteoblasts. Clin Oral Investig. 2012; 16:1153–1159.
13. Viereck V, Emons G, Lauck V, Frosch K-H, Blaschke S, Gründker C, Hofbauer LC. Bisphosphonates pamidronate and zoledronic acid stimulate osteoprotegerin production by primary human osteoblasts. Biochem Biophys Res Commun. 2002; 291:680–686. [PubMed: 11855844]
14. Bellido T, Plotkin LI. Novel actions of bisphosphonates in bone: Preservation of osteoblast and osteocyte viability. Bone. 2011; 49:50–55. [PubMed: 20727997]
15. Plotkin LI, Weinstein RS, Parfitt AM, Roberson PK, Manolagas SC, Bellido T. Prevention of osteocyte and osteoblast apoptosis by bisphosphonates and calcitonin. J Clin Invest. 1999; 104:1363–1374. [PubMed: 10562298]
16. Boanini E, Torricelli P, Gazzano M, Fini M, Bigi A. The effect of zoledronate-hydroxyapatite nanocomposites on osteoclasts and osteoblast-like cells in vitro. Biomaterials. 2012; 33:722–730. [PubMed: 22014461]
17. Boanini E, Torricelli P, Gazzano M, Fini M, Bigi A. The effect of alendronate doped calcium phosphates on bone cells activity. Bone. 2012; 51:944–952. [PubMed: 22878156]

18. Boanini E, Torricelli P, Gazzano M, Fini M, Bigi A. Crystalline calcium alendronate obtained by octacalcium phosphate digestion: a new chance for local treatment of bone loss diseases? Adv Mater. 2013 Advance online publication.
19. Altman GH, et al. Cell differentiation by mechanical stress. FASEB J. 2002; 16:270–272. [PubMed: 11772952]
20. Bhumiratana S, Grayson WL, Castaneda A, Rockwood DN, Gil ES, Kaplan DL, Vunjaknovakovic G. Nucleation and growth of mineralized bone matrix on silk-hydroxyapatite composite scaffolds. Biomaterials. 2011; 32:2812–2820. [PubMed: 21262535]
21. Sengupta S, Park S-H, Seok GE, Patel A, Numata K, Lu C-L, Kaplan DL. Quantifying osteogenic cell degradation of silk biomaterials. Biomacromolecules. 2010; 11:3592–3599. [PubMed: 21105641]
22. Kim U-J, Park J, Kim HJ, Wada M, Kaplan DL. Three-dimensional aqueous-derived biomaterial scaffolds from silk fibroin. Biomaterials. 2005; 26:2775–2785. [PubMed: 15585282]
23. Jin H-J, Park J, Karageorgiou V, Kim U-J, Valluzzi R, Cebe P, Kaplan DL. Water-stable silk films with reduced β-sheet content. Adv Funct Mater. 2005; 15:1241–1247.
24. Janković I, Prstojević D, Marinković V. Spectrophotometric determination of alendronate in pharmaceutical formulations via complex formation with Fe(III) ions. J Pharm Biomed Anal. 2002; 28:1215–1220. [PubMed: 12049986]
25. Taha EA, Youssef NF. Spectrophotometric determination of some drugs for osteoporosis. Chem Pharm Bull. 2003; 51:1444–1447. [PubMed: 14646329]
26. Petersson IU, Löberg JEL, Fredriksson AS, Ahlberg EK. Semi-conducting properties of titanium dioxide surfaces on titanium implants. Biomaterials. 2009; 30:4471–4479. [PubMed: 19524291]
27. Mills OP, Rose WI. Shape and surface area measurements using scanning electron microscope stereo-pair images of volcanic ash particles. Geosphere. 2010; 6:805–811.
28. Chen X, Ostadi H, Jiang K. Three-dimensional surface reconstruction of diatomaceous frustules. Anal Biochem. 2010; 403:63–66. [PubMed: 20382100]
29. Ostadi H, Jiang K, Prewett PD. Characterisation of FIB milling yield of metals by SEM stereo imaging technique. Microelectron Eng. 2009; 86:1021–1024.
30. Meinel L, et al. Silk implants for the healing of critical size bone defects. Bone. 2005; 37:688–698. [PubMed: 16140599]
31. Kirker-Head C, et al. BMP-silk composite matrices heal critically sized femoral defects. Bone. 2007; 41:247–255. [PubMed: 17553763]
32. Mandal BB, Grinberg A, Gil ES, Panilaitis B, Kaplan DL. High-strength silk protein scaffolds for bone repair. Proc Natl Acad Sci U S A. 2012; 109:7699–7704. [PubMed: 22552231]
33. Moreau JE, Anderson K, Mauney JR, Nguyen T, Kaplan DL, Rosenblatt M. Tissue-engineered bone serves as a target for metastasis of human breast cancer in a mouse model. Cancer Res. 2007; 67:10304–10308. [PubMed: 17974972]
34. Goldstin R, Reagan M, Anderson K, Kaplan D. Human bone marrow – derived MSCs can home to orthotopic breast cancer tumors and promote bone metastasis. Cancer Res. 2010; 70:10044–10050. [PubMed: 21159629]
35. Sun L, Wang X, Kaplan DL. A 3D cartilage - inflammatory cell culture system for the modeling of human osteoarthritis. Biomaterials. 2011; 32:5581–5589. [PubMed: 21565399]
36. Rogers MJ. From molds and macrophages to mevalonate: a decade of progress in understanding the molecular mode of action of bisphosphonates. Calcif Tissue Int. 2004; 75:451–461. [PubMed: 15332174]
37. Kellinsalmi M, Mönkkönen H, Mönkkönen J, Leskelä H-V, Parikka V, Hämäläinen M, Lehenkari P. In vitro comparison of clodronate, pamidronate and zoledronic acid effects on rat osteoclasts and human stem cell-derived osteoblasts. Basic Clin Pharmacol Toxicol. 2005; 97:382–391. [PubMed: 16364054]
38. Kasting GB, Francis MD. Retention of etidronate in human, dog, rat. J Bone Miner Res. 1992; 7:513–522. [PubMed: 1615760]
39. Duque G, Rivas D. Alendronate has an anabolic effect on bone through the differentiation of mesenchymal stem cells. J Bone Miner Res. 2007; 22:1603–1611. [PubMed: 17605634]

40. Im G-I, Qureshi SA, Kenney J, Rubash HE, Shanbhag AS. Osteoblast proliferation and maturation by bisphosphonates. Biomaterials. 2004; 25:4105–4115. [PubMed: 15046901]

41. Idris AI, Rojas J, Greig IR, Van't Hof RJ, Ralston SH. Aminobisphosphonates cause osteoblast apoptosis and inhibit bone nodule formation in vitro. Calcif Tissue Int. 2008; 82:191–201. [PubMed: 18259679]

42. Idris AI, Greig IR, Bassonga-Landao E, Ralston SH, van't Hof RJ. Identification of novel biphenyl carboxylic acid derivatives as novel antiresorptive agents that do not impair parathyroid hormone-induced bone formation. Endocrinology. 2009; 150:5–13. [PubMed: 18772231]

43. García-Moreno C, et al. Effect of alendronate on cultured normal human osteoblasts. Bone. 1998; 22:233–239. [PubMed: 9580147]

44. Boanini E, Torricelli P, Gazzano M, Giardino R, Bigi A. Alendronate-hydroxyapatite nanocomposites and their interaction with osteoclasts and osteoblast-like cells. Biomaterials. 2008; 29:790–796. [PubMed: 18022226]

45. Silverman SL, Watts NB, Delmas PD, Lange JL, Lindsay R. Effectiveness of bisphosphonates on nonvertebral and hip fractures in the first year of therapy: the risedronate and alendronate (REAL) cohort study. Osteoporos Int. 2007; 18:25–34. [PubMed: 17106785]

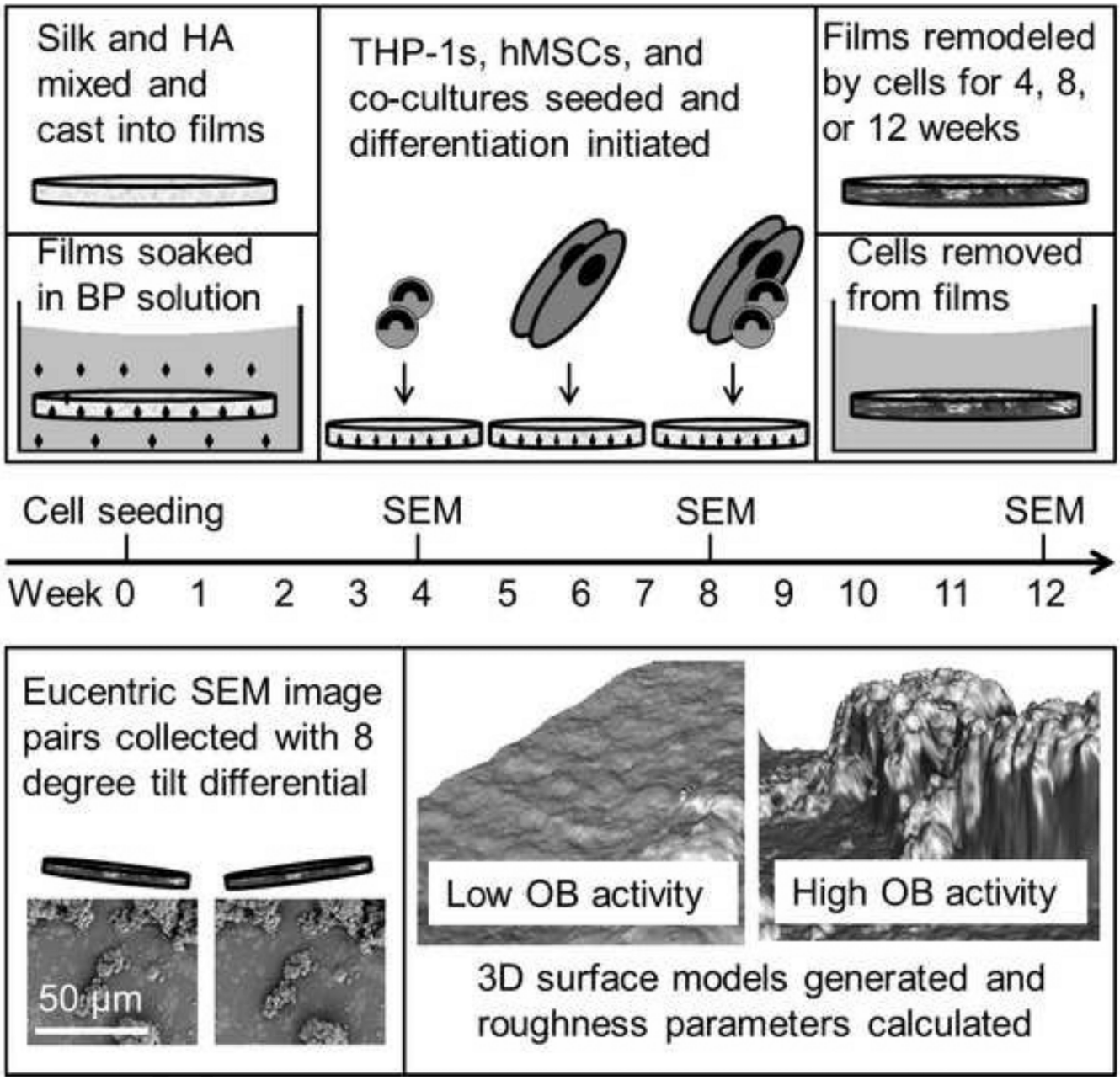

Figure 1. Schematic of 12 week studies

Top: Films were cast from a dispersion of HA in aqueous silk solution. Following drying and water annealing, films were soaked in solutions of clodronate or alendronate which bound to the HA. Following autoclaving, films were seeded with hMSCs, THP-1s, or a co-culture of the two cell types in equal number. Differentiation was then initiated, and films were remodeled by cells for 4, 8, or 12 weeks. For surface metrology analysis cells were removed from films by soaking in water overnight at 4°C and films were dried and sputter coated. Bottom: Eucentric SEM images were taken with an 8 degree difference in tilt angle. 3D surface models were generated and roughness parameters were calculated. Example surfaces from low and high osteoblast activity (approximately 600 μm^2) are shown.

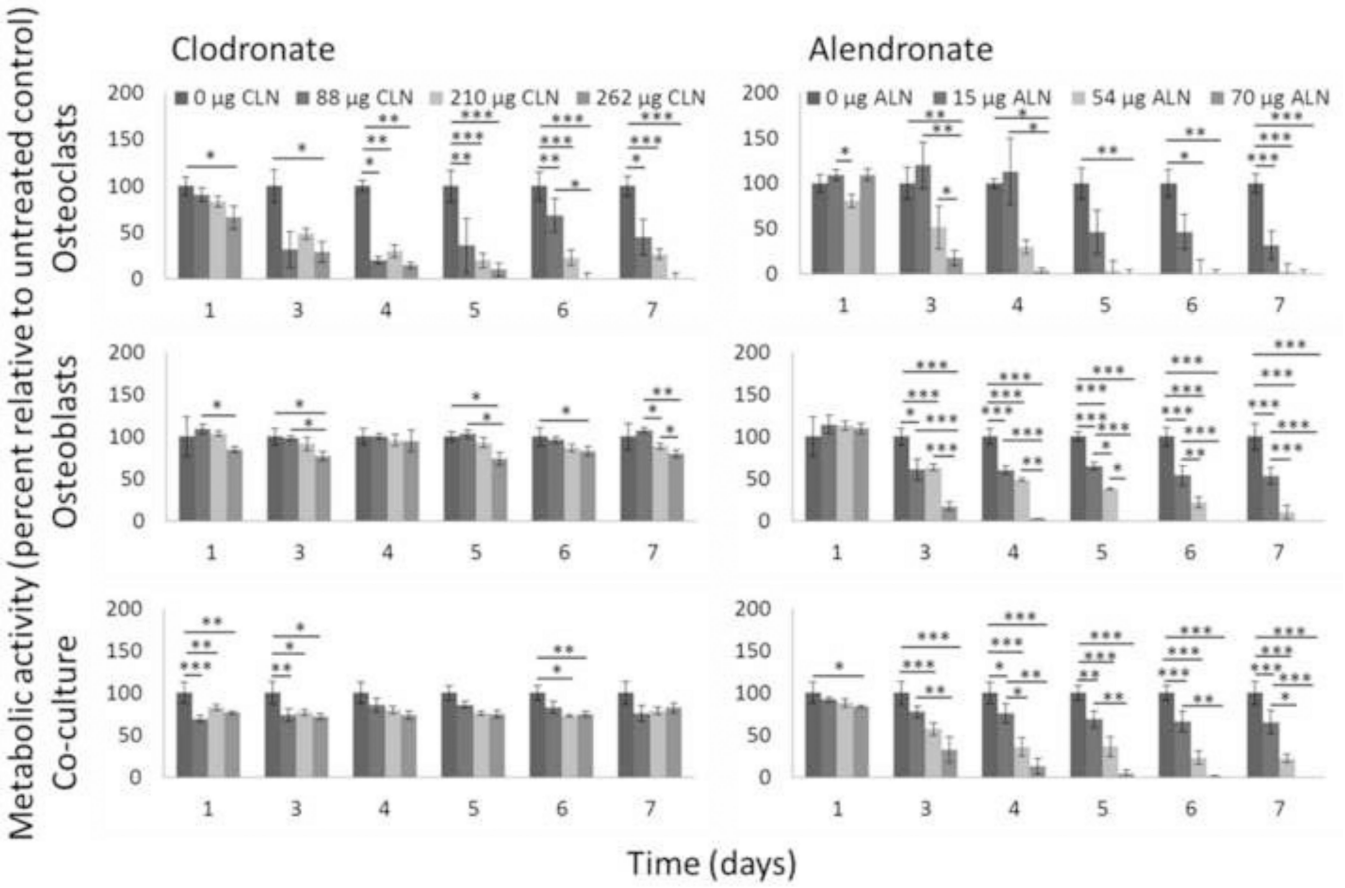

Figure 2. Effects of bisphosphonates on metabolic activity (7 days)

THP-1 osteoclasts, hMSC osteoblasts, or a co-culture of the two cell types were maintained on silk-HA films or silk-HA films loaded with clodronate or alendronate for 7 days, and metabolic activity was measured by Alamar Blue. Metabolic activity of cells grown on drug-loaded films is normalized to metabolic activity of the same cell type(s) grown on control silk-HA films and is expressed as mean ± SD. Top left: Osteoclasts cultured on clodronate-loaded films. Top right: Osteoclasts cultured on alendronate-loaded films. Middle left: Osteoblasts cultured on clodronate-loaded films. Middle right: Osteoblasts cultured on alendronate-loaded films. Bottom left: Co-cultures cultured on clodronate-loaded films. Bottom right: Co-cultures cultured on alendronate-loaded films. *$p<0.05$, **$p<0.01$, ***$p<0.001$.

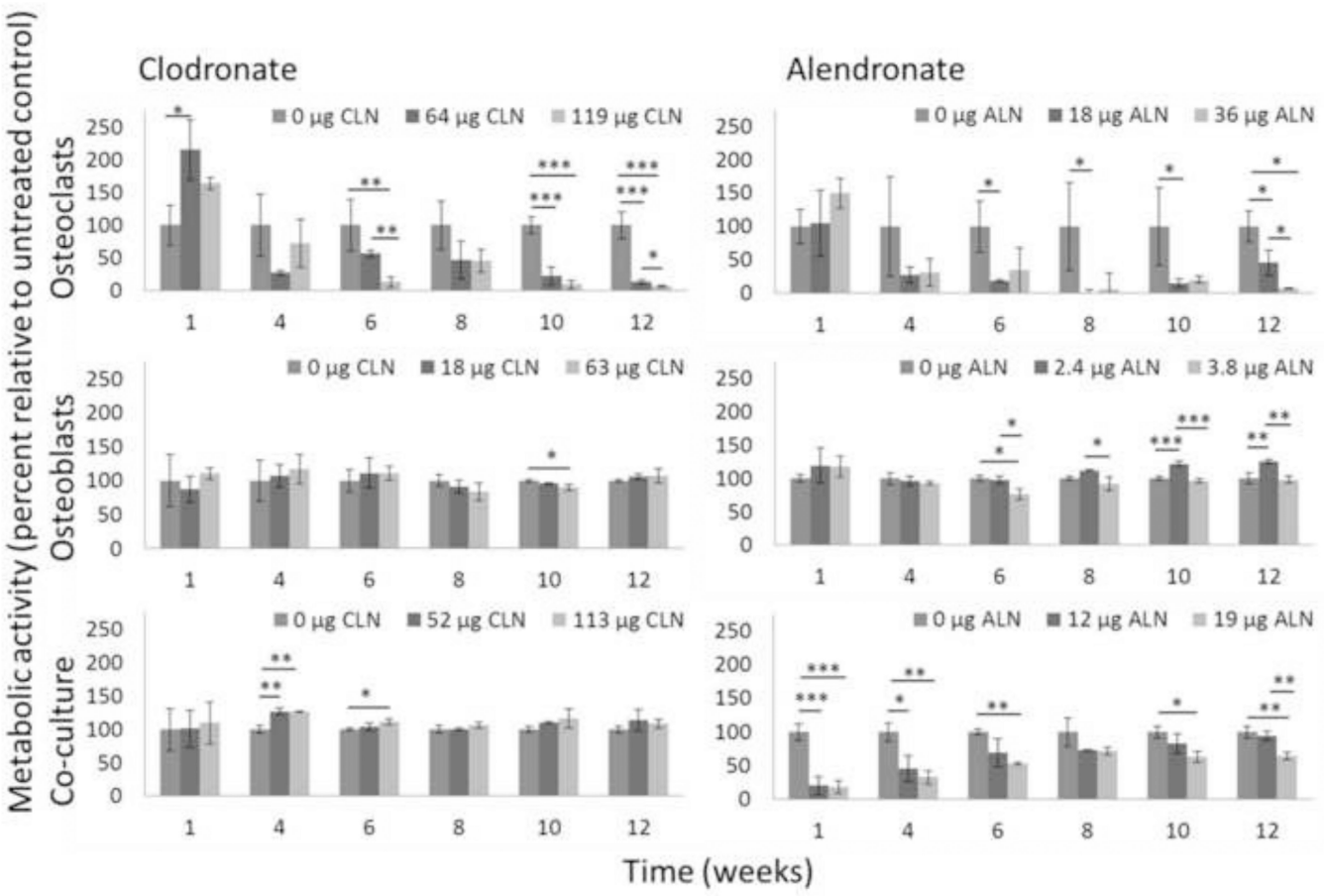

Figure 3. Effects of bisphosphonates on metabolic activity (12 weeks)

THP-1 osteoclasts, hMSC osteoblasts, or a co-culture of the two cell types were maintained on silk-HA films or silk-HA films loaded with clodronate or alendronate for 12 weeks, and metabolic activity was measured by Alamar Blue. Metabolic activity of cells grown on drug-loaded films is normalized to metabolic activity of the same cell type(s) grown on control silk-HA films and is expressed as mean ± SD. Top left: Osteoclasts cultured on clodronate-loaded films. Top right: Osteoclasts cultured on alendronate-loaded films. Middle left: Osteoblasts cultured on clodronate-loaded films. Middle right: Osteoblasts cultured on alendronateloaded films. Bottom left: Co-cultures cultured on clodronate-loaded films. Bottom right: Co-cultures cultured on alendronate-loaded films. *p<0.05, **p<0.01, ***p<0.001.

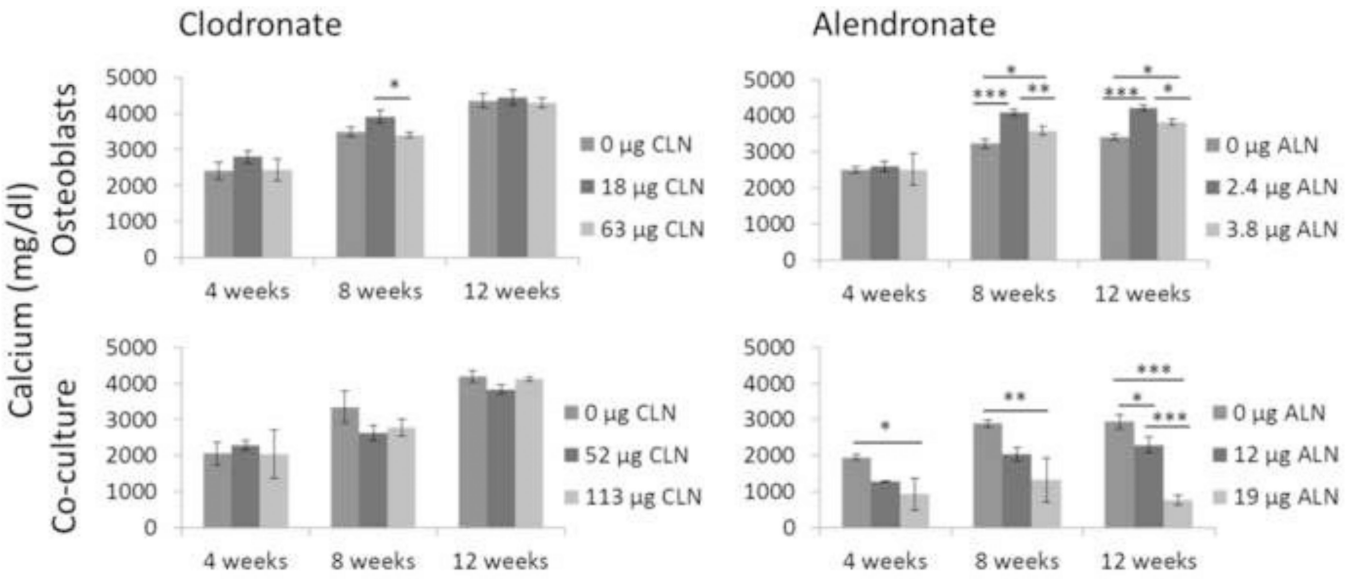

Figure 4. Effects of bisphosphonates on calcium deposition

Calcium content of films was measured after 4, 8, and 12 weeks of culture and expressed as mean ± SD. Top left: Osteoblasts cultured on clodronate-loaded films. Top right: Osteoblasts cultured on alendronate-loaded films. Bottom left: Co-cultures cultured on clodronate-loaded films. Bottom right: Co-cultures cultured on alendronate-loaded films. *p<0.05, **p<0.01, ***p<0.001.

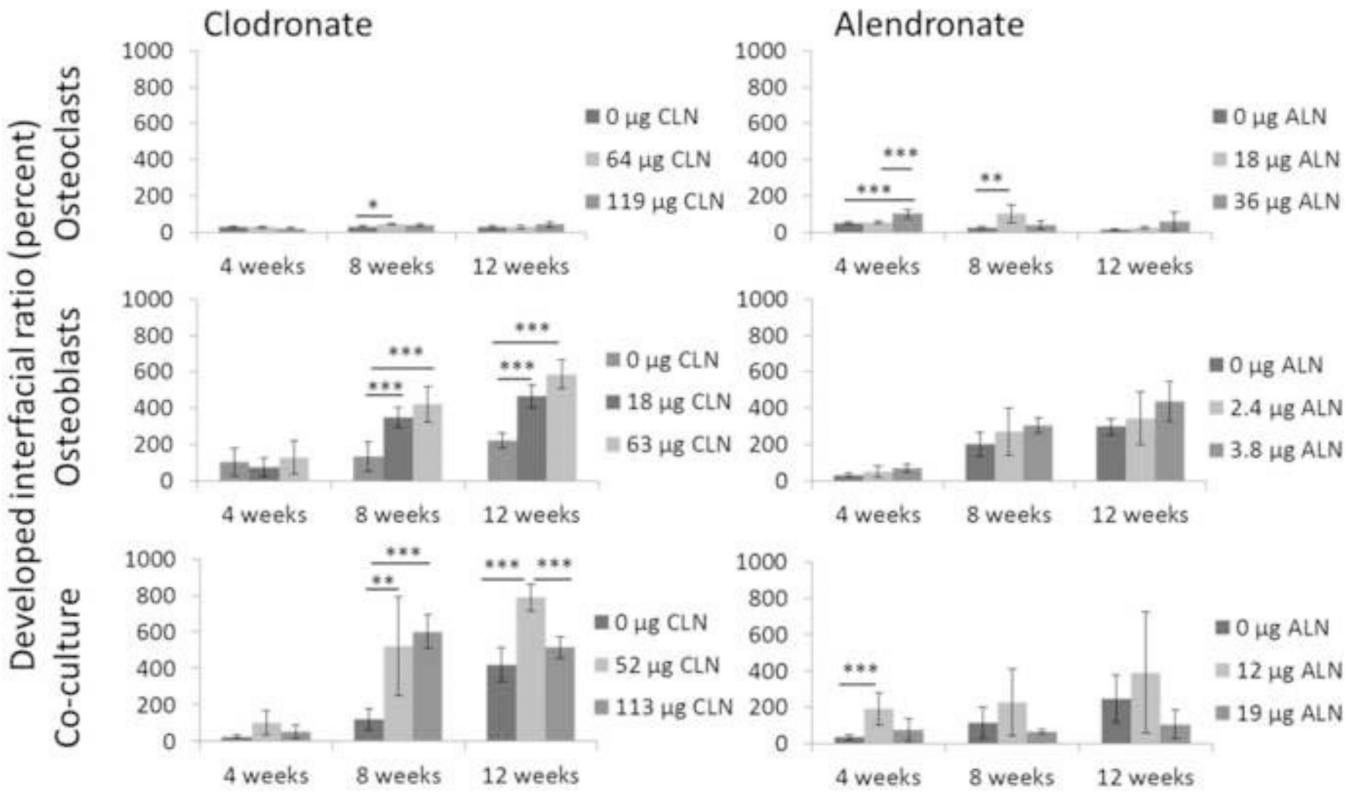

Figure 5. Effects of bisphosphonates on developed interfacial ratio

3D surfaces were reconstructed from SEM imaging and the developed interfacial ratio (Sdr) was calculated after 4, 8, and 12 weeks of culture and expressed as mean ± SD. Top left: Osteoclasts cultured on clodronate-loaded films. Top right: Osteoclasts cultured on alendronate-loaded films. Middle left: Osteoblasts cultured on clodronate-loaded films. Middle right: Osteoblasts cultured on alendronate-loaded films. Bottom left: Co-cultures cultured on clodronate-loaded films. Bottom right: Co-cultures cultured on alendronate-loaded films. *p<0.05, **p<0.01, ***p<0.001.

Table 1

Bisphosphonate soaking solutions for long term study

Silk-HA films were soaked in solutions which contained 82 to 800 μg clodronate per film or 7 to 136 μg alendronate per film. Following soaking, the amounts of bisphosphonates remaining in the soaking solution were measured and the amount bound per film was calculated.

		Osteoclasts		Osteoblasts		Co-cultures		Average
		Low	High	Low	High	Low	High	
Clodronate	μg/film soaking solution	400	800	82	410	246	615	
	Percentage bound to film	16%	15%	22%	15%	21%	18%	18%
	μg/film bound	64	119	18	63	52	113	
Alendronate	μg/film soaking solution	68	136	7	14	37	75	
	Percentage bound to film	26%	26%	34%	27%	32%	25%	29%
	μg/film bound	18	36	2.4	3.8	12	19	

Table 2
Effects of bisphosphonates on osteoclasts and osteoblasts

The mechanisms by which bisphosphonates induce osteoclast apoptosis are relatively well-understood, but the effects on osteoblasts have received less attention and are more complicated. At low doses, both non-nitrogenous and nitrogenous bisphosphonates prevent osteoblast apoptosis, but higher doses inhibit proliferation and differentiation and cause apoptosis.

Bisphosphonate type	Cell type	Mechanism	Downstream effects
Non-nitrogenous	Osteoclasts	Toxic ATP analogues	Apoptosis [7]
	Osteoblasts (low doses)	Connexin 43 channels and ERK phosphorylation	Protection against corticosteroid-induced apoptosis [15]
	Osteoblasts (high doses)	Toxic ATP analogues?	Decreased survival [37]
Nitrogenous	Osteoclasts	FPPS inhibition and blocked protein prenylation	Decreased functionality and apoptosis [8]
	Osteoblasts (low doses)	Connexin 43 channels and ERK phosphorylation	Protection against corticosteroid-induced apoptosis [15]
	Osteoblasts (high doses)	FDPS inhibition and blocked protein prenylation	Decreased functionality and apoptosis [41]
	Osteoblasts (high doses)	Independent of protein prenylation	Decreased bone nodule formation [41]